Magnetic phase boundaries of $CsMnF_3$: XY-to-Ising crossover and the virtual bicritical point

Y. Shapira
Francis Bitter National Magnet Laboratory, Massachusetts Institute of Technology, Cambridge, Massachusetts 02139

N. F. Oliveira, Jr.
Francis Bitter National Magnet Laboratory, Massachusetts Institute of Technology, Cambridge, Massachusetts 02139 and Instituto de Fisica, Universidade de São Paulo, C.P. 20516, São Paulo, Brasil

T. S. Chang*
Francis Bitter National Magnet Laboratory, Massachusetts Institute of Technology, Cambridge, Massachusetts 02139

(Received 17 September 1979)

The ordering temperature T_c of the easy-plane hexagonal antiferromagnet $CsMnF_3$ was measured as a function of magnetic field H, up to 120 kOe. T_c was determined from the thermal expansion anomaly at constant H. At $H=0$, $T_N \equiv T_c(0) = 51.4$ K. When $\vec{H}$ is in the hexagonal plane, the boundary $T_c(H)$ is bow shaped: with increasing H, T_c first increases, then passes through a maximum, and later decreases. The maximum T_c is ~37 mK above T_N, and it occurs at $H \cong 29.5$ kOe. The bow-shaped phase boundary is attributed to the XY-to-Ising crossover which is induced by the magnetic field, as discussed by Fisher, Nelson, and Kosterlitz. Fits to the phase boundary $T_c(H)$ give a crossover exponent $\phi = 1.185 \pm 0.03$ for one sample and $\phi = 1.184 \pm 0.025$ for another, compared to the theoretical value $\phi(n=2) = 1.175 \pm 0.015$. When $\vec{H}$ is perpendicular to the hexagonal plane, T_c decreases monotonically with increasing H, but the decrease is not in accordance with mean-field theory, which predicts a decrease proportional to H^2. The deviation from mean-field behavior is attributed to a virtual bicritical point (VBP) with Heisenberg symmetry, which exists mathematically at a negative value of H^2. Although the VBP cannot be observed directly, it affects the behavior in the observable region of $H^2 \geq 0$. Physically, a magnetic field applied perpendicular to the easy plane enhances the Heisenberg-to-XY symmetry breaking, which at $H=0$ is solely due to the weak easy-plane uniaxial anisotropy. The enhanced symmetry breaking causes a non-mean-field dependence of T_c on H. An equation derived on this basis gives a good description of the phase boundary $T_c(H)$. This equation contains three adjustable parameters, two of which can also be estimated without recourse to the phase boundary $T_c(H)$. The values for these two parameters obtained from a best fit to $T_c(H)$ agree with the independent estimates.

I. INTRODUCTION

Second-order phase transitions are divided into universality classes.[1] Each universality class has its own critical exponents and scaling functions. In the last decade, attention has focused on situations in which a small perturbation $\mathcal{H}_1$ breaks the symmetry of the original Hamiltonian $\mathcal{H}_0$, and thereby causes a change of the universality class. The perturbation $\mathcal{H}_1$ is then said to cause a "crossover" between two universality classes.

In many cases the universality class is determined by only three factors: the lattice dimensionality d, the spin dimensionality (or number of components of the order parameter) n, and the range of the interaction. Within this subset of cases, a crossover occurs when the perturbation $\mathcal{H}_1$ changes either d, or n, or the range of the interaction. In the present paper we are concerned with a crossover due to a change of n, the lattice dimensionality ($d=3$) and the range of the interaction (short) are assumed to be fixed. In particular, we study the effect of a crossover due to a change in n on the ordering temperature T_c of the antiferromagnet $CsMnF_3$.

The basic theory of such crossover effects in weakly anisotropic antiferromagnets is that of Fisher, Nelson, and Kosterlitz (FNK).[2-4] Earlier, similar crossover effects in ferromagnets were discussed theoretically by Riedel and Wegner,[5] Pfeuty *et al.*,[6] and others.[7] The first detailed experimental test of the FNK predictions was carried out by Rohrer,[8] who studied the bicritical point in $GdAlO_3$. References to later experimental works on the bicritical point of several antiferromagnets, and on the phase boundaries of isotropic antiferromagnets, can be found in a recent review.[9] This review, and also Ref. 10, outline some of the results of the present work. Monte Carlo calculations of phase boundaries near the bicritical

point, and of isotropic antiferromagnets, were carried out by Landau and Binder.[11]

In many antiferromagnets, a change in the spin dimensionality can be produced by applying a magnetic field $\vec{H}$. Physically, the magnetic field favors configurations for which the staggered magnetization $\vec{L}$ is perpendicular to $\vec{H}$. Thus, the field suppresses that component $L_{\parallel}$ of $\vec{L}$ which is parallel to $\vec{H}$. In a simple three-dimensional fully isotropic antiferromagnet, the transition at $H=0$ is Heisenberg-like ($n=3$), because all three components of the order parameter $\vec{L}$ are involved in the transition. The H-induced suppression of $L_{\parallel}$ then leads to an XY-like transition ($n=2$) at finite H. Thus, for a fully isotropic antiferromagnet the application of a magnetic field leads to a crossover from Heisenberg symmetry to XY symmetry. According to FNK, this crossover is similar to that discussed earlier for ferromagnets,[5,6] with H^2 playing the role of the symmetry-breaking parameter g. The extended scaling hypothesis[6] implies that as g increases from zero, T_c should increase by an amount proportional to $g^{1/\phi}$, for small g, where ϕ is the crossover exponent. Thus one consequence of the theory is that in a fully isotropic antiferromagnet, T_c should increase with increasing H, for low H. For very low H, the increase of T_c should be proportional to $H^{2/\phi}$. This prediction is in a striking contrast to mean-field theory in which T_c decreases with increasing H. Measurements of the H dependence of T_c in the isotropic antiferromagnet $RbMnF_3$ confirmed the prediction of FNK.[12,13] The experimentally determined ϕ in $RbMnF_3$ is in good agreement with the predicted value $\phi(n=3)=1.25$ for a Heisenberg-to-XY crossover.

In the present work we studied the phase boundaries $T_c(H)$ of the easy-plane antiferromagnet $CsMnF_3$, in which the anisotropy in the easy plane is extremely small. Neglecting this in-plane anisotropy, the transition at $H=0$ is XY-like because only the two spin components in the easy plane become critical. The situation at finite H is illustrated in Fig. 1. When $\vec{H}$ is perpendicular to the easy plane, no particular direction in that plane is singled out, and the transition remains XY-like. On the other hand, if $\vec{H}$ is the easy plane the component $\vec{L}$ which is parallel to $\vec{H}$ is suppressed, and the transition becomes Ising-like ($n=1$). The XY-to-Ising crossover in the latter situation affects the H dependence of T_c. According to FNK, the phase boundary $T_c(H)$ when $\vec{H}$ is in the easy plane (and for low H) should be given by

$$T_c(H)-T_N=aH^{2/\phi}-bH^2 \ , \qquad (1)$$

where $T_N=T_c(0)$ is the Néel temperature, a and b are positive constants, and $\phi=\phi(n=2)$. The predicted value for ϕ ($n=2$) is 1.175 ± 0.015.[6] The two terms on the right-hand side of Eq. (1) have the following meanings. The term $aH^{2/\phi}$ represents the effect of the crossover on T_c. This term is analogous to the term $(\text{const})(g^{1/\phi})$ in the theory of crossover in ferromagnets.[5,6] By itself, this term leads to an increase of T_c with increasing H. The second term, $-bH^2$, is a mean-field-like term which appears in the theory of FNK as the leading nonlinear correction to scaling.[4] This term will be discussed in Sec. VI D. By itself, the term $-bH^2$ leads to a decrease of T_c with increasing H. The competition between the two terms, $aH^{2/\phi}$ and $-bH^2$, leads to a bow-shaped phase boundary $T_c(H)$; as H increases from zero, T_c first increases, then passes through a maximum, and later decreases.

When $\vec{H}$ is perpendicular to the easy plane of an antiferromagnet, the transition remains XY-like. Then, in the strict sense, the magnetic field does not induce a crossover from one symmetry to another. Nevertheless, if the uniaxial anisotropy which favors the easy plane is very small compared to the exchange energy, the phase boundary $T_c(H)$ will depart from mean-field behavior. The physical reason for this departure is similar to that which causes a non-mean-field behavior when a genuine crossover takes place. This reason is basically the following. A uniaxial anisotropy of the easy-plane type suppresses the criticality of the spin component which is perpen-

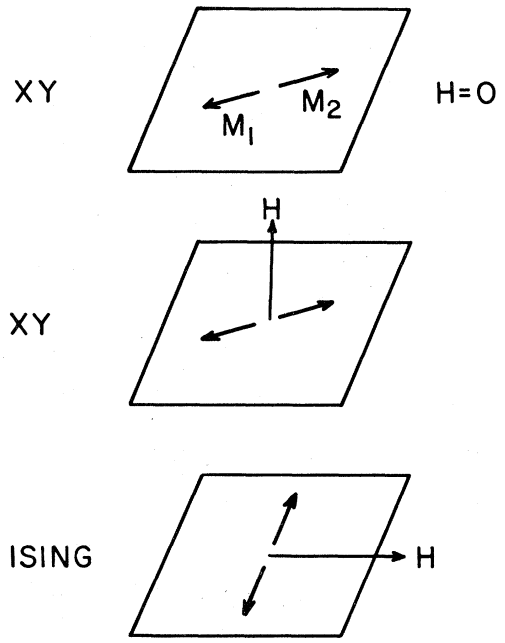

FIG. 1. Schematic illustrating the configurations of the sublattice magnetizations $\vec{M}_1$ and $\vec{M}_2$ of a simple uniaxial easy-plane antiferromagnet for: $H=0$; $\vec{H}$ perpendicular to the easy plane; and $\vec{H}$ in the easy plane. The tipping of $\vec{M}_1$ and $\vec{M}_2$ toward the direction of $\vec{H}$ is neglected. The symmetry of the ordering transition is indicated.

dicular to the easy plane. For a weak anisotropy, the degree of suppression is relatively small. A magnetic field, applied perpendicular to the easy plane, enhances the suppression of the same spin component (i.e., the out-of-plane component, which is parallel to $\vec{H}$). This enhanced suppression has an effect on the phase boundary $T_c(H)$. That is, the boundary is no longer given by the mean-field expression (for low H)

$$T_c(H) - T_N = -b^* H^2 \ , \tag{2}$$

where b^* is a positive constant. In Refs. 9 and 10 we introduced the concept of the virtual bicritical point to account quantitatively for the phase boundary when $\vec{H}$ is perpendicular to the easy plane. Here we present a fuller discussion of the virtual bicritical point in $CsMnF_3$. In addition we present the data for the phase boundary when $\vec{H}$ is in the easy plane, and show that these data are in good agreement with the FNK theory for the case of an XY-to-Ising crossover.

This paper is arranged as follows. In Sec. II, the relevant properties of $CsMnF_3$ are discussed. In Sec. III, the experimental techniques used to determine the phase boundaries $T_c(H)$ are outlined. The results for T_c vs H, for $\vec{H}$ both in the easy plane and perpendicular to it, are presented in Sec. IV. In Sec. V, the phase boundary $T_c(H)$ for $\vec{H}$ in the easy plane is analyzed quantitatively, and is compared to the FNK prediction for an XY-to-Ising crossover. An experimental value for the crossover exponent $\phi\,(n=2)$ is obtained. The phase boundary for $\vec{H}$ perpendicular to the easy plane, and the virtual bicritical point, are discussed in Sec. VI.

II. SOME PROPERTIES OF $CsMnF_3$

$CsMnF_3$ is a hexagonal crystal with symmetry which is described by the D_{6h}^4 space group. The unit cell contains six Mn^{++} ions, two of which occupy sites with one local symmetry (A sites), and four others occupy sites with a different local symmetry (B sites). The magnetic properties of $CsMnF_3$ were first investigated by Lee *et al.*,[14] and later by others.[15–20] These investigations showed that the material is an antiferromagnet below $T_N \cong 53$ K. (Our own value for T_N is somewhat lower, as discussed later.) The antiferromagnetic order may be described as a series of ferromagnetic layers, perpendicular to the hexagonal axis [0001], with the spins in adjacent layers pointing in opposite directions. Thus, the six spins in the unit cell, on the A and B sites, have the following orientations relative to each other: $A(+)$, $B(-)$, $B(+)$, $A(-)$, $B(+)$, and $B(-)$. In the ordered phase, and when $H=0$, the spins lie in the hexagonal plane.

The earliest analysis of the magnetic properties of $CsMnF_3$, by Lee *et al.*,[14] used a simple two-sublattice model in which the distinction between the A and the B sites was overlooked. This analysis led to the following values at $T=0$: The exchange field is $H_E = 3.5 \times 10^5$ Oe. The uniaxial anisotropy field is $H_A = -7500$ Oe, where the minus sign indicates that the anisotropy favors the (0001) plane rather than the [0001] axis. The anisotropy field in the hexagonal plane is $H_a = 1.1$ Oe. In some later analyses of the magnetic data, the distinction between the A and B sites was explicitly taken into account, and a four-sublattice model was used. One such analysis, by Yamaguchi and Sakuraba,[19] led to exchange fields of 7.9×10^5 and 4.7×10^5 Oe for the A and B sites. Antiferromagnetic resonance data[18] indicated that the actual gap in the high-frequency branch of the spin-wave spectrum is $|2H_E H_A|^{1/2} = 41$ kOe, rather than the value 72 kOe obtained from the values for H_E and H_A given by Lee *et al.* Finally we mention that the value $H_a = 1.1$ Oe of Lee *et al.* is the highest quoted in the literature. Apparently, sample imperfections and small strains can affect the (very small) in-plane anisotropy field H_a. At any rate, H_a/H_E is smaller than 10^{-5}.

The possibility of a canted magnetic moment in $CsMnF_3$ was discussed in the literature. The thermodynamic potential of an antiferromagnet is often expressed as a Landau-type expansion in powers of the staggered magnetization and of the magnetization. The symmetry of $CsMnF_3$ forbids the existence of the lowest-order term which can give rise to a canted magnetic moment in an antiferromagnet.[18,21] However, the symmetry allows a higher-order term which gives rise to a canted moment along the [0001] direction when the staggered magnetization is near some directions in the (0001) plane.[21] Evidence for such a canting of the spins on the B sites was reported by Mil'ner and Popkov who performed magneto-optic measurements on $CsMnF_3$.[22] However, both magnetization and resonance measurements show no evidence whatsoever for a net canted moment. To reconcile the latter data with their own conclusions, Mil'ner and Popkov considered the possibility that the spins on the A sites are canted in the opposite direction, leading to a compensated structure with zero net canted moment. A model for a compensated-moment structure in $CsMnF_3$ was discussed later by Gredeskul and Mil'ner.[23] In the interpretation of our data we shall assume that there is no net canted moment.

The ordering transition of $CsMnF_3$, at $H=0$, should belong to the XY $d=3$ universality class. Evidence in support of this prediction was presented by Ikeda[20] who performed specific-heat measurements. The data suggested that when $CsMnF_3$ was cooled toward T_N, a crossover from a Heisenberg behavior to an XY behavior took plane as T approached T_N.

III. EXPERIMENTAL TECHNIQUES

A. Samples

Experiments were conducted on three single crystals of $CsMnF_3$, grown by the Crystal Physics Group, Center for Materials Science and Engineering, MIT. The Czochralski technique was used. Each of the samples was x rayed, and then cut and lapped to a rectangular parallelepiped. A typical linear dimension was 6 mm. The faces of each of the samples were the (0001), $(10\bar{1}0)$, and $(1\bar{2}10)$ crystallographic faces. The three samples will be referred to as No. 1, No. 2, and No. 3.

B. Thermal expansion measurements

The ordering temperature $T_c(H)$ was determined from thermal-expansion measurements. The length $l(H,T)$ of the sample was measured as a function of T at constant H. A capacitance dilatometer, made of copper, was used to measure the change in l.[24] The data for l vs T were recorded on a punch tape, which was subsequently fed into a computer for processing. Figure 2(a) is an example of l vs T data, taken in this case at $H=0$. To determine the transition, the data were differentiated numerically, to obtain the thermal expansion coefficient $\Gamma=(1/l)(\partial l/\partial T)$.

Because Γ is proportional to one of the second derivatives of the thermodynamic potential $\Phi(T,H,p_x,p_y,p_z)$, where p_i is a uniaxial pressure, the ordering transition appears as a λ anomaly in Γ vs T. The λ anomaly at the Néel temperature, obtained by differentiating the data in Fig. 2(a), is shown in Fig. 2(b). This example covers a temperature range of several degrees. Usually, data were taken only over a range of several tenths of a degree near $T_c(H)$. A typical example is shown in Fig. 3(a). An expanded view of the same data in the vicinity of the maximum of the λ anomaly is shown in Fig. 3(b).

Ideally, a λ anomaly with a sharp maximum at $T_c(H)$ should be present. In practice, the peak of the λ anomaly is rounded both by the nonideality of the sample and by the numerical differentiation of l with respect to T. (The derivative $\partial l/\partial T$ is obtained from a fit of l vs T over a finite temperature interval.) Because of the rounding, the precise identification of the transition temperature is difficult. We used either of the following two criteria to locate T_c: (i) $T_c=T_{max}$, where T_{max} is the temperature at which Γ is maximum, and (ii) $T_c=T_{ext}$, where the extrapolated temperature T_{ext} is at the intersection of the two tangents at the inflection points of the Γ vs T curve [see Fig. 3(b)]. The value of T_c depended on the criterion which was used; the two criteria led to T_c's which differed by several mK. However, the difference $T_c(H)-T_N$ did not show any systematic dependence on the criterion. We used both criteria in the analysis of each set of experimental data. However, the results obtained using the criterion $T_c=T_{ext}$ were given a greater weight because usually T_{ext} could be determined with greater precision.

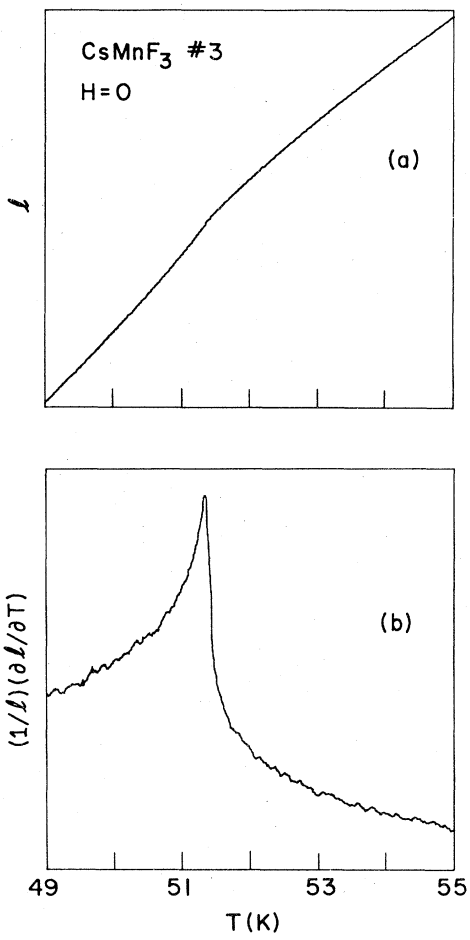

FIG. 2. Thermal expansion of $CsMnF_3$ (at $H=0$) near the Néel temperature T_N. (a) The length l of the sample (measured along the $[11\bar{2}0]$ direction) as a function of temperature T. (b) The thermal-expansion coefficient, $(1/l)(\partial l/\partial T)$, as a function of T. The thermal expansion of the sample is always measured relative to that of the copper capacitance cell.

In a typical experimental run, some 10–20 sets of l vs T data were taken at various values of H. Of these sets of data, five were usually taken at $H=0$. For nonzero H, two sets of l vs T data were usually taken at the same H. The reason for taking more sets of data at $H=0$ was that any error in $T_N=T_c(0)$ propagated to all final values of $T_c(H)-T_N$, whereas an error in a particular $T_c(H)$ affected only one final value of $T_c(H)-T_N$.

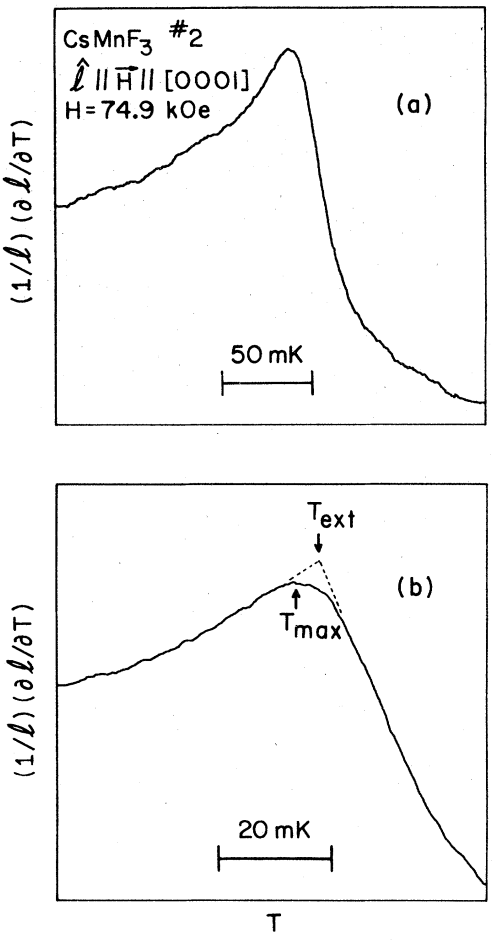

FIG. 3. T dependence of the thermal-expansion coefficient $(1/l)(\partial l/\partial T)$ for a fixed magnetic field, $H=74.9$ kOe, directed parallel to the [0001] axis. The unit vector $\hat{l}$ indicates the crystallographic direction along which l was measured. (a) Results for a comparatively wide temperature range. (b) Expanded view of the results near the maximum. T_{max} is the temperature at the maximum of $(1/l)(\partial l/\partial T)$, and T_{ext} is the temperature at the intercept of the two tangents at the inflection points on both sides of the maximum.

C. Thermometry

High-precision thermometry at high magnetic fields was essential in these experiments. We used thermistor resistance thermometers attached directly to the samples with G.E. 7031 varnish. The experimental setup, and the methods used to correct for the small magnetoresistance of the thermometers were described earlier.[9] The precision of T in the present experiments was ~ 1 mK, or $\sim 2\times 10^{-5}$ for T/T_N.

D. Magnetic fields

Two different magnets were used in the present experiments: a Bitter-type water-cooled magnet with fields up to 120 kOe, and a NbTi superconducting magnet with a maximum field of 88 kOe. The data in sample No. 1 were taken in the Bitter magnet, whereas the data in samples No. 2 and and No. 3 were taken in the superconducting magnet. The advantage of the Bitter magnet was the higher field. The advantage of the superconducting magnet was that it was free from the slight mechanical vibration of the Bitter magnet (caused by the cooling water). The absence of vibrations reduced the noise of the dilatometer, which, in turn, improved the precision of the results for $T_c(H)-T_N$. This led to smaller rms deviations of the data points from the best fits which described the phase boundaries.

All values of the magnetic field were corrected for the demagnetizing field. The magnitude of the demagnetizing field was between 0.2% and 0.3% of the applied field, depending on the shape of the particular sample and its orientation in the field. All values of H which are quoted below are for the internal magnetic field.

IV. EXPERIMENTAL RESULTS

A. Néel temperature

The Néel temperature T_N was determined from the λ anomaly in the thermal-expansion coefficient $\Gamma(T)$ at $H=0$. The thermal expansion was measured along both the [0001] and $[10\bar{1}0]$ crystallographic directions in sample 1, along the [0001] direction in sample 2, and along the $[11\bar{2}0]$ direction in sample 3. The values for T_N are 51.38 ± 0.02, 51.38 ± 0.02, and $51.38_5\pm0.02$ K for samples 1, 2, and 3, respectively. Here, the uncertainties represent the absolute accuracy, rather than the precision.

B. Phase boundaries for $\vec{H}\perp[0001]$

The dependence of the ordering temperature T_c on H, for $\vec{H}$ in the easy plane, was measured in samples 1 and 3. For sample 1, $\vec{H}$ was parallel to the $[10\bar{1}0]$ direction. For sample 3, $\vec{H}$ was parallel to the $[11\bar{2}0]$ direction. The data for $T_c(H)-T_N$ as a function of H are shown in Fig. 4. An expanded view of the low-H portion of the same data is shown in Fig. 5. The results in Figs. 4 and 5 indicate that the phase boundaries for $\vec{H}\parallel[10\bar{1}0]$ and for $\vec{H}\parallel[11\bar{2}0]$ are identical, within the experimental precision.

The striking feature of the phase boundary (for $\vec{H}$ in the easy plane) is that it is bow shaped. That is, as H increases continuously from zero, T_c first in-

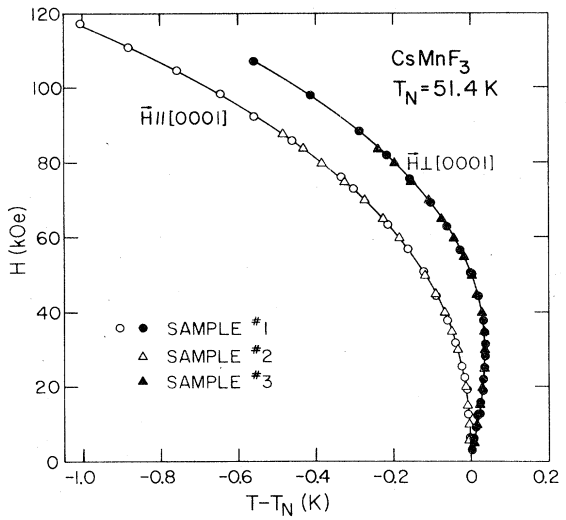

FIG. 4. Phase boundaries, T_c vs H, of $CsMnF_3$ for $\vec{H}$ parallel and perpendicular to the hexagonal axis [0001]. The solid line for $\vec{H}\perp[0001]$ is the best fit to Eq. (1) of the data points for sample 1. The solid line for $\vec{H}\parallel[0001]$ is the best fit to Eq. (7) of the data points for sample 1. The best fits are discussed in the text.

creases, and only later decreases. The maximum value of T_c is approximately 37 mK above T_N, and it occurs at approximately 29.5 kOe. On a reduced temperature scale, $t=(T-T_N)/T_N$, the maximum of $T_c(H)$ is at $t=7\times10^{-4}$. The fact that the phase boundary is bow shaped is attributed to the XY-to-Ising crossover, as discussed in Sec. I. A detailed analysis is given in Sec. V.

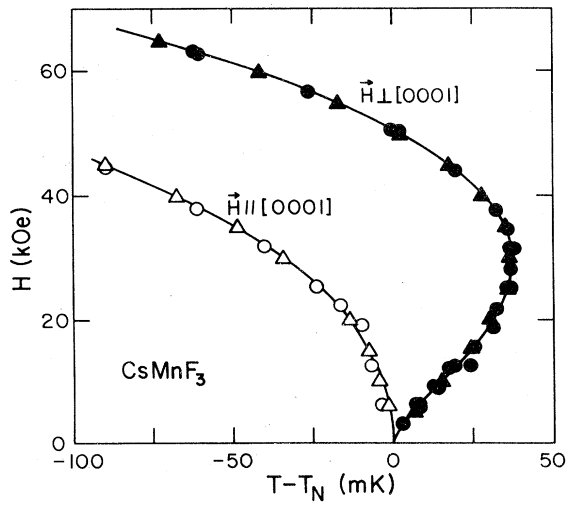

FIG. 5. Expanded view of the low-H portion of Fig. 4.

C. Phase boundary for $\vec{H}\parallel[0001]$

The phase boundary for $\vec{H}$ parallel to the [0001] direction (i.e., perpendicular to the easy plane) was measured in both samples 1 and 2. The results are shown in Fig. 4. An expanded view of the low-H portion of these data is shown in Fig. 5. Note that the data for the two samples are in very good agreement with each other, and that the phase boundary for this direction of $\vec{H}$ is not bow shaped. That is, T_c decreases monotonically with increasing H. A detailed analysis of these data is presented in Sec. VI.

V. XY-ISING CROSSOVER

In this section the phase boundary for $\vec{H}$ in the easy plane is compared with the FNK theory. This comparison is preceded by comments concerning our value for the Néel temperature.

A. Néel temperature

Our value for the Néel temperature $T_N=51.4$ K, is lower than those quoted by other workers. Lee *et al.*[14] give $T_N=53.5$ K, based on the temperature where the torque vanishes. Yamaguchi and Sakuraba[19] quote $T_N=53.5\pm0.5$ K from susceptibility measurements. Borovik-Romanov *et al.*[18] obtained $T_N=53.6\pm0.3$ K from the temperature dependence of the antiferromagnetic resonance (AFMR) frequency. Finally, Ikeda[20] quotes $T_N=53.06\pm0.02$ K, based on a fit to his specific-heat data. In spite of these earlier results, we feel confident that our value for T_N is accurate, at least for our samples. We have checked the calibration of the platinum resistance thermometer used in the determination of T_N, and have ruled out the possibility of an error of order of 2 K. Also, the data in Fig. 2, and other similar data, give no indication of a second transition near 53 K.

Some of the disagreement concerning T_N might have been caused by inaccurate experimental criteria for identifying T_N. Not all standard methods of determining T_N are accurate. An often-used procedure for determining T_N is from the maximum of the susceptibility χ as a function of T. Modern theory indicates, however, that the maximum of $\chi(T)$ occurs above T_N. Thus, we tend to doubt the accuracy of a determination of T_N from susceptibility measurements (unless one focuses on the T dependence of the derivative $\partial\chi/\partial T$, which is expected to have a maximum at T_N). The identification of T_N as the temperature where the torque vanishes is also questionable. Many antiferromagnets have anisotropic susceptibilities in the paramagnetic phase and at T_N, so that the torque is nonzero at $T=T_N$. The value of T_N quoted by Borovik-Romanov *et al.* is also suspect because these authors found that the AFMR

linewidth, plotted as a function of T, exhibited a λ peak approximately 2 K below their value for T_N. That is, the linewidth had a maximum near 51.6 K, which is close to *our* value for T_N. Borovik-Romanov *et al.* stated that they had no reasonable explanation as to why the maximum linewidth occurred ~2 K below T_N. We feel that it is possible that the maximum of the linewidth occurred, in fact, at T_N. The only clear disagreement with our value for T_N is the specific-heat data of Ikeda which show a λ peak at 53 K.

B. Crossover exponent ϕ from the phase boundary for $\vec{H}$ in the easy plane

The phase boundary $T_c(H)$ for $\vec{H} \| [10\bar{1}0]$ is identical to that for $\vec{H} \| [11\bar{2}0]$, within experimental accuracy. This observation is consistent with the extremely low in-plane anisotropy of $CsMnF_3$.

The most striking feature of the phase boundary $T_c(H)$ is that it is bow shaped. This feature is attributed to the *XY*-to-Ising crossover which is caused by the field H. According to the FNK theory, the phase boundary (in the absence of anisotropy in the easy plane) should be given by Eq. (1), with $\phi = \phi(n=2)$. Least-squares fits of the data to Eq. (1) were performed, treating a and b as adjustable parameters but keeping ϕ fixed at its theoretical value $\phi(n=2) = 1.175$. The results for the data sets in samples 1 and 3 (with $\vec{H} \| [10\bar{1}0]$ and $\vec{H} \| [11\bar{2}0]$, respectively) are given in Table I.

A sensitive test of the theory is whether the experimentally-derived ϕ agrees with the predicted value $\phi(n=2) = 1.175$. For this purpose, least-squares fits to Eq. (1) were made, treating ϕ as well as a and b as adjustable parameters. The results of separate fits to the data in samples 1 and 3 are given in Table II. In these fits, all the data points for a given sample were used. As can be seen, the values of ϕ derived from these fits are in good agreement with the theory. In Figs. 4 and 5, the solid line for the boundary with $\vec{H} \perp [0001]$ is the least-squares fit for sample 1. The best fit for sample 3 is very nearly the same.

TABLE I. Results of least-squares fits to Eq. (1) of the data for $\vec{H} \perp [0001]$. Here, a and b are treated as adjustable parameters, while ϕ is held fixed at its theoretical value $\phi(n=2) = 1.175$. For these fits, H is in units of kOe, and T is in units of mK. The numbers in parentheses are the standard deviations in units of the last quoted decimal place, e.g., 0.7827(32) is 0.7827 ±0.0032. δT is the rms deviation (in mK) between the measured $T_c(H) - T_N$ and the best fit.

Sample No.	a	b	δT
1	0.7827(32)	0.2428(9)	1.48
3	0.7792(19)	0.2421(5)	0.45

TABLE II. Results of least-squares fits to Eq. (1) of the data for $\vec{H} \perp [0001]$. Here, ϕ as well as a and b are treated as adjustable parameters. H is in units of kOe, and T is in units of mK. The numbers in parentheses are the standard deviations in units of the last quoted decimal place, e.g., 0.7855(110) is 0.7855 ±0.0110. δT is the rms deviation (in mK) between the measured $T_c(H) - T_N$ and the best fit.

Sample No.	a	b	ϕ	δT
1	0.7855(110)	0.2397(110)	1.178(11)	1.48
3	0.7865(69)	0.2324(77)	1.184(7)	0.42

We have also carried out least-squares fits in which only data points $T_c(H)$ in the range $0 < H < H_R$ were included. That is, starting from a data set for a given sample, all data points with $H > H_R$ were deleted, and a fit to Eq. (1) was made treating a, b, and ϕ as adjustable parameters. Successive fits were made for different H_R. The results for ϕ as a function of H_R in sample 1 are shown in Fig. 6. The error bars in this figure are typical standard deviations for $\phi(H_R)$, i.e., each error bar gives $\pm\sigma_\phi$. The theoretical values for $\phi(n=2)$ and $\phi(n=3)$ are shown as dashed lines. Note that the experimental results are in better agreement with the theoretical value of $\phi(n=2)$, as expected. Based on the results in Fig. 6 (including the results for H_R's lower than the maximum field) our best estimate of ϕ, for sam-

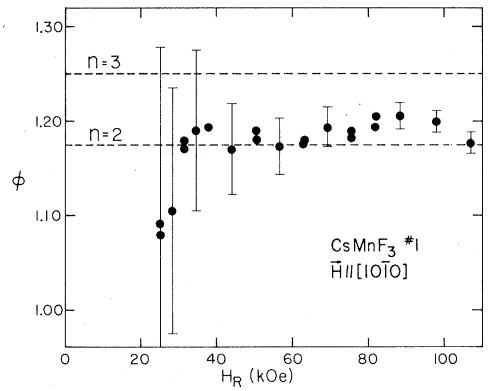

FIG. 6. Crossover exponent ϕ obtained from fits to Eq. (1) of the $T_c(H)$ data in sample 1, with $\vec{H} \| [10\bar{1}0]$. Each point represents the result of a fit of the data in the range $0 < H < H_R$. Error bars are typical standard deviations, $\pm\sigma_\phi$. Horizontal dashed lines are the theoretical values of ϕ for $n=2$ and $n=3$.

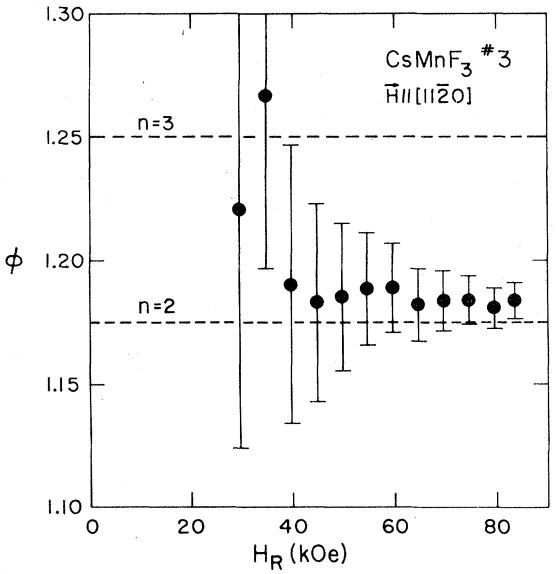

FIG. 7. Crossover exponent ϕ obtained from fits to Eq. (1) of the $T_c(H)$ data in sample 3, with $\vec{H} \parallel [11\bar{2}0]$. Each point represents the results of a fit for data in the range $0 < H < H_R$. Error bars are standard deviations, $\pm\sigma_\phi$. The horizontal dashed lines are the theoretical values of ϕ for $n = 2$ and 3.

ple 1 with $\vec{H} \parallel [10\bar{1}0]$, is $\phi = 1.185 \pm 0.03$.

Similar results for ϕ as a function of H_R in sample 3 are shown in Fig. 7. Again, the agreement with the theoretical value for $\phi(n=2)$ is better than with that for $\phi(n=3)$. Our best estimate of ϕ, for sample 3 with $\vec{H} \parallel [11\bar{2}0]$, is $\phi = 1.184 \pm 0.025$. The quoted uncertainty is our estimated overall uncertainty, and is larger than the standard deviation σ_ϕ for high H_R (which is approximately 0.01).

C. Comments concerning the in-plane anisotropy

In the preceding analysis, which was based on Eq. (1), we assumed that there was no anisotropy in the easy plane. To estimate the effect of the small in-plane anisotropy on the experimentally-derived values of ϕ, we followed an approach similar to that used in the earlier work on $RbMnF_3$ (Sec. V C of Ref. 13). This approach is based on the following reasoning. In the absence of an in-plane anisotropy, the staggered magnetization $\vec{L}$ for any nonzero $\vec{H}$ (applied in the easy plane) is perpendicular to $\vec{H}$. When a small in-plane anisotropy is present, the application of a magnetic field leads to a rotation of $\vec{L}$ toward that direction in the easy plane which is perpendicular to $\vec{H}$. However, for finite H_a the configuration $\vec{L} \perp \vec{H}$ is reached only at a field H_c of order $(H_E H_a)^{1/2}$. Earlier data on $CsMnF_3$ indicated that H_c was equal to several hundred Oe at 4.2 K.[14,19] In the present work we determined H_c from magnetostriction measurements similar to those performed earlier on $RbMnF_3$.[25] The magnetostriction was measured with the same dilatometer and in the same experimental configuration as in the thermal-expansion measurements used to determine $T_c(H)$. The only difference was that in the magnetostriction measurements the length l of the sample was measured as a function of H at constant T, whereas in the thermal-expansion measurements T was varied at constant H. The magnetostriction data gave $H_c \cong 0.6$ kOe at 4.2 K, for both sample 1 (with $\vec{H} \parallel [10\bar{1}0]$) and sample 3 (with $\vec{H} \parallel [11\bar{2}0]$). For both samples, the value of H_c at temperatures slightly below T_N also was approximately 0.6 kOe.

The effect of the in-plane anisotropy on the experimentally-derived ϕ was estimated by assuming that a spin-flop transition occurred at $H_c(T)$. Then the boundary $T_c(H)$ for $H > H_c(T \cong T_N) = H_b$ represents the boundary between the spin-flop phase and the paramagnetic phase. The theory for such a phase boundary was discussed by FNK in connection with the problem of the bicritical point.[2-4] Comparison of the phase boundary with this theory was made on the basis of Eq. (6) of Ref. 13. The data for $H > H_b$ were fitted to this equation, treating a^*, b^*, and ϕ and the bicritical temperature T_b as adjustable parameters, but holding the bicritical field H_b fixed at 0.6 kOe. The values of ϕ obtained from such fits to the data in samples 1 and 3 differed by ~ 0.01 from those quoted above. This change of ϕ is less than half the final uncertainties in the values of ϕ quoted above. Thus, the error in ϕ caused by neglecting the in-plane anisotropy was small.

The in-plane anisotropy in our samples is believed to have two origins. First, there is the intrinsic sixfold anisotropy of the material, with an anisotropy field of ~ 1 Oe or less. For a pure fourfold anisotropy, the theory[26] indicates that H_c vanishes at T_N. We expect the same for a pure sixfold anisotropy. Because in our samples H_c did not vanish at T_N, we believe that another source of in-plane anisotropy was present in addition to the intrinsic sixfold anisotropy. As discussed in Ref. 25, the measurements with our capacitance dilatometers are carried out with the sample subjected to a small uniaxial pressure p which is created by the springs which hold the sample in place. It was shown in Sec. IV B 5 of Ref. 25 that for the cubic antiferromagnet $RbMnF_3$, a uniaxial pressure applied parallel to the [001] crystallographic direction created an effective uniaxial anisotropy. An analogous treatment shows that a uniaxial pressure applied along any direction in the hexagonal plane of $CsMnF_3$ creates a uniaxial in-plane anisotropy. The observed longitudinal magnetostriction in $CsMnF_3$ is an H-induced elongation, which occurs as $\vec{L}$ rotates toward that direction in the easy plane which is perpendicular to $\vec{H}$. At 4.2 K, the magnitude of the elongation is $\Delta l/l \cong 2 \times 10^{-6}$. The sign of the mag-

netostriction indicates that a uniaxial compression in the hexagonal plane tends to rotate $\vec{L}$ toward the axis of the compression. Let $H_a(p)$ be the stress-induced in-plane uniaxial anisotropy field. Then, the magnitude of the magnetostriction and the known value of the uniaxial pressure in our experiments ($\sim$7 bar) lead to the order-of-magnitude estimate $H_a(p) \sim 0.1$ Oe at 4.2 K. This estimate was made assuming a simple two-sublattice model. In our experiments the axis of the compression was parallel to $\vec{H}$, so that the easy axis of the stress-induced anisotropy was parallel to $\vec{H}$.

The stress-induced uniaxial anisotropy is expected to increase H_c, because the additional preference of $\vec{L}$ to be aligned parallel to $\vec{H}$ must be overcome. In contrast to the cases of pure fourfold or sixfold anisotropies, the value of H_c near T_N is expected to remain finite because a small uniaxial anisotropy of the easy-axis type leads to a finite bicritical field H_b. The value of H_c near T_N is expected to increase with increasing uniaxial pressure. This was confirmed in recent experiments[27] on $RbMnF_3$ which showed that $H_c(T \cong T_N)$ increased as the uniaxial pressure exerted on the sample in the dilatometer was increased. The expected order of magnitude of H_b will be discussed in Sec. VI D 1. For the stress-induced uniaxial anisotropy in our experiments on $CsMnF_3$ we expect $H_b \sim [2H_E H_a(p)]^{1/2} \cong 0.3$ kOe. This is comparable to the observed value $H_c \cong 0.6$ kOe near T_N.

It should be noted that the precise origin of the in-plane anisotropy, which led to a finite value of H_c near T_N, is unimportant as far as the estimate of the effect of this anisotropy on our values for ϕ.

VI. VIRTUAL BICRITICAL POINT

A. Phase boundary for $\vec{H} \| [0001]$

The motivation for introducing the concept of the virtual bicritical point comes from an examination of the phase boundary, T_c vs H, for $\vec{H} \| [0001]$. As noted in Sec. I, for this orientation of $\vec{H}$ there is no change in the spin dimensionality, i.e., the transition has XY symmetry both at $H=0$ and at finite H. On this basis one might have expected that the phase boundary near T_N would be given by the mean-field expression for $T_c(H)$ near T_N, Eq. (2). Figure 8 shows a plot of T_c as a function of H^2 for sample 2. It is clear that T_c is not linear in H^2, so that Eq. (2) is not obeyed. Plots of T_c vs H^2 for sample 1, which were presented earlier in Refs. 9 and 10, led to the same conclusion. Note that Figs. 4 and 5 indicate that the data in samples 1 and 2 are in good agreement with each other.

We now show that the nonlinearity of T_c as a function of H^2 is not caused by an unintentional misalignment of $\vec{H}$ relative to the [0001] crystallographic axis.

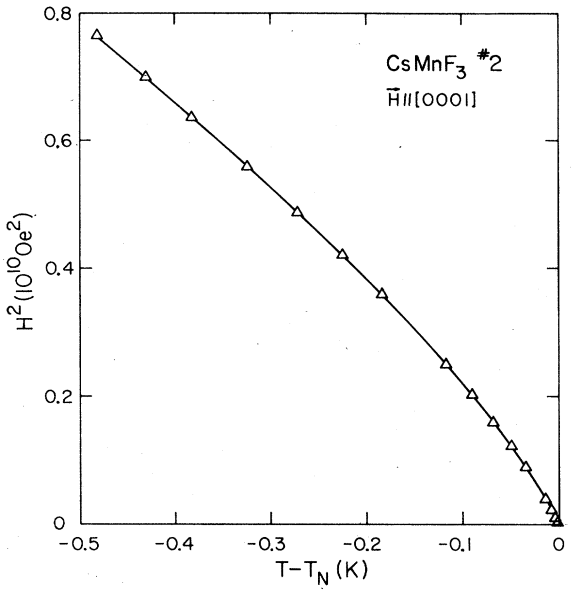

FIG. 8. Phase boundary $T_c(H^2)$ for sample 2 when $\vec{H}$ is parallel to the [0001] axis. Note that the ordinate is H^2. The solid line is the best fit to Eq. (7). The best fit was obtained by holding ϕ fixed at $\phi(n=3)=1.25$, but treating A, B, and h_0 as adjustable parameters.

For the sake of argument, suppose that for $\vec{H}$ exactly parallel to the [0001] axis T_c was linear in H^2, as in Eq. (2). A misalignment angle θ between $\vec{H}$ and the [0001] axis should then have two effects on the phase boundary: (i) The field component $H\sin\theta$ in the (0001) plane would lead to an XY-to-Ising crossover. This symmetry breaking should add a term to the dependence of T_c on H. This term is expected to be approximated by the form $\Delta T_c \propto g^{1/\phi}$, where $g \propto H^2 \sin^2\theta$ and $\phi = \phi\ (n=2) \cong 1.175$. (ii) The coefficient b^* in the mean-field term $-b^* H^2$, should be slightly θ dependent. The combination of these two effects would then lead to an expression of the form

$$T_c(H) - T_N = a^*(H^2 \sin^2\theta)^{1/\phi} - b^* H^2 \ . \qquad (3)$$

Note that when $\theta = 90°$, Eq. (3) reduces to Eq. (1). We expect a^* not to vary appreciably with θ. Thus, we expect a^* to be approximately equal to the coefficient a obtained by fitting the phase boundary for $\vec{H} \perp [0001]$ to Eq. (1).

The nonlinearity of T_c vs H^2, due to the misalignment, is given by the first term on the right-hand side of Eq. (3). In our experiments, the misalignment angle is estimated to be smaller than 3°. Taking $\theta = 3°$, we calculated the phase boundary expected from Eq. (3). Here we chose a^* to be equal to any of the values of a in Tables I or II, and chose a value for b^* which gave a rough overall agreement with the

observed phase boundary for $\vec{H} \| [0001]$. The nonlinearity of the calculated curve, T_c vs H^2, was then found to be far too small to account for the observed nonlinearity in Fig. 8. We then asked what value of θ would give the best agreement between the data in Fig. 8 and Eq. (3). A least-squares fit in which ϕ was held fixed at 1.175, a^* was held fixed at the value of a in Tables I and II (approximately 0.78), and θ and b^* were treated as adjustable parameters, gave $\theta = 35°$. A similar fit to the data for sample No. 1, which extend to higher H, gave $\theta = 42°$. These values for the misalignment angle θ are an order of magnitude larger than the estimated maximum misalignment angle. Moreover, the fits to Eq. (3) gave rms deviations δT (between the measured T_c's and the best fit) which were several times the estimated experimental uncertainties. The large δT's reflect the fact that Eq. (3) leads to an initial increase of T_c with increasing H, which is contrary to the observed behavior for $\vec{H} \| [0001]$. In other words, a field misalignment should lead to a bow-shaped phase boundary, which is not observed. We thus conclude that the nonlinearity of T_c vs H^2 in Fig. 8 is not due to field misalignment.

B. Virtual bicritical point

The intrinsic anisotropy of $CsMnF_3$ (i.e., anisotropy at $H=0$) is mainly due to dipole-dipole interactions, with a smaller contribution from crystalline fields.[14] To an excellent approximation, this intrinsic anisotropy is a pure uniaxial easy-plane anisotropy. This implies that the transition at the Néel point is XY-like; only the two spin components in the (0001) plane undergo critical fluctuations. However, the fluctuations of the third spin component should be quite strong (even though they do not become critical) because the anisotropy energy is only of order 1% of the exchange energy. That is, the lowering of the symmetry from an Heisenberg to an XY symmetry is caused by a fairly weak symmetry-breaking parameter g. When a magnetic field $\vec{H}$ is applied parallel to the [0001] axis, it prefers configurations with $\vec{L}$ in the (0001) plane. Thus, the magnetic field enhances the suppression of the spin fluctuations parallel to [0001]; i.e., the magnetic field increases g.

We attribute the nonlinear dependence of T_c on H^2, for $\vec{H} \| [0001]$, to the H-induced enhancement of the Heisenberg-to-XY symmetry breaking. Our basic strategy for obtaining an explicit expression for the dependence of T_c on H is to relate the present problem to a similar problem which has already been solved. The solved problem is that of the Heisenberg-to-XY crossover. Such a crossover was considered in anisotropic ferromagnets,[5,6] and near the bicritical point (BP) of a cylindrically-symmetric easy-axis antiferromagnet.[2–4] In the latter case, the Heisenberg-to-XY crossover occurs when H is increased beyond the bicritical field H_b. The major difference between an easy-plane and an easy-axis antiferromagnet is that in the former it is not possible to reach the special critical point of Heisenberg symmetry by applying a (real) magnetic field.

To relate the case of easy-plane anisotropy to the FNK theory we used two slightly different approaches. In the first,[9] a thought experiment was performed in which the intrinsic anisotropy was made to disappear. This resulted in a Heisenberg-like transition at $H=0$. It was then imagined that the anisotropy increased from zero up to its actual value in the crystal. This led to an increase of g from zero to g_0. Subsequently, the magnetic field was turned on, which caused a further increase of g. The main assumption made in Ref. 9 was that the H-induced change of g (at constant intrinsic anisotropy) was proportional to H^2, as in the FNK theory for an easy-axis anitferromagnet. That is,

$$g = g_0 + cH^2 \ , \tag{4}$$

where c is a positive constant. An equation for $T_c(H)$ was then obtained using extended scaling,[5,6] which implies

$$T_c(g) - T_c(0) = A^* g^{1/\phi} \ , \tag{5}$$

where A^* is a positive constant. In the final expression for T_c vs H we have also added a mean-field-like correction term, $\Delta T_c = -BH^2$. This correction term is similar to that in the FNK theory, where it appears as a result of choosing an optimal scaling axis $\tilde{t}=0$.[3] The correction term will be discussed more fully in Sec. VI D 2. The final expression for T_c vs H, for small H, is

$$T_c(H) - T_N = A^*[(g_0 + cH^2)^{1/\phi} - g_0^{1/\phi}] - BH^2 \ , \tag{6}$$

where $\phi = \phi(n=3) \cong 1.25$, and A^* and B are positive constants which depend on the material.

In the standard treatment of Heisenberg-to-XY crossover, the Heisenberg point is the point where $g=0$. Equation (4) therefore implies that, formally, the Heisenberg point occurs at a negative value of H^2, namely, $H^2 = -g_0/c \equiv -h_0^2$. This observation leads to an alternative approach to the problem. In this second approach,[10] a formal similarity is sought between the case of an easy-plane antiferromagnet and the case of a cylindrically-symmetric easy-axis antiferromagnet. This formal similarity is achieved when the range of H^2 in the easy-plane case is allowed to extend beyond the physically allowed range of $H^2 \geq 0$ to the physically forbidden range of negative H^2. For weak easy-plane anisotropy, this formal procedure leads to the phase diagram in Fig. 9(b). This phase diagram should be compared to the phase diagram in Fig. 9(a) which sketches the FNK results for an easy-axis antiferromagnet. In Fig. 9, the sym-

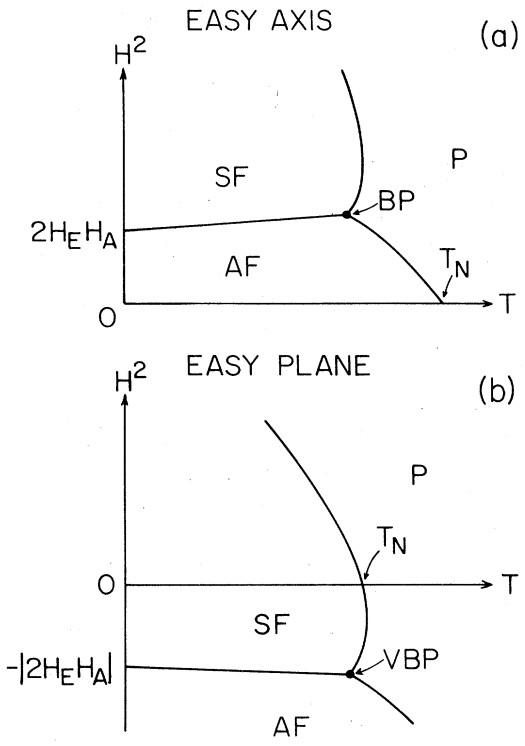

FIG. 9. Schematic of the phase boundaries, in the $T-H^2$ plane, for (a) a uniaxial easy-axis antiferromagnet and for (b) a uniaxial easy-plane antiferromagnet. In both cases $\vec{H}$ is parallel to the symmetry axis. Note that the virtual bicritical point (VBP) in (b) is below the observable region of $H^2 \geq 0$.

bols P, AF, and SF stand for the paramagnetic, antiferromagnetic, and spin-flop phases, respectively. The AF-SF transition is also known as the spin-flop transition.

Those transitions in Fig. 9(b) which occur at negative H^2 we call virtual transitions. In particular, the Heisenberg-like critical point where the three phase boundaries meet is called a virtual bicritical point (VBP) in analogy with the ordinary BP in an easy-axis antiferromagnet. As is the case for the ordinary BP, g varies linearly with H^2 near the VBP. That is, $g \propto (H^2 - H_{VB}^2)$, where $H_{VB}^2 \equiv -h_0^2$ is the value of H^2 at the VBP.[28] When the uniaxial easy-plane anisotropy is small in magnitude, the VBP is close to the $H^2=0$ axis, and the influence of the VBP on the observable phase boundary should be noticeable at small positive H^2. That is, T_c will not be linear in H^2. The formal approach in Ref. 10 leads to the following expression for the phase boundary for small positive H^2,

$$T_c(H) - T_N = A[(H^2 + h_0^2)^{1/\phi} - h_0^{2/\phi}] - BH^2 \ , \quad (7)$$

where $\phi = \phi(n=3)$, and A and B are positive constants. Equation (7) is equivalent to Eq. (6) with $h_0^2 = g_0/c$, $A = A^* c^{1/\phi}$.

In what follows, we compare the data with Eq. (7), emphasizing those aspects which were not discussed (or only briefly mentioned) in Refs. 9 and 10.

C. Least-squares fits to Eq. (7)

The data for T_c vs H, with $\vec{H} \| [0001]$, were fitted to Eq. (7) by the least-squares method. In these fits, ϕ was held fixed at its theoretical value $\phi(n=3) = 1.25$, but A, B, and h_0 were treated as adjustable parameters. Separate fits were made to the data sets for samples 1 and 2. The results are given in Table III. The best fit to the data in sample 2 is shown in Fig. 8 as a solid line. It is clear that Eq. (7) provides a good description of this set of data. The best fit for sample 1 was shown in Refs. 9 and 10, and is also shown in Figs. 4 and 5 of the present paper. Because the data in samples 1 and 2 are in good agreement with each other, the best fits for these two data sets are very close to each other.

D. Discussion of the least-squares fits

The good agreement of the data for $\vec{H} \| [0001]$ with Eq. (7) is, in itself, evidence in support of the explanation of these data in terms of the VBP. Additional supportive evidence is provided by considering the numerical values of the parameters obtained from the fits to this equation. Of the three adjustable parameters (A, B, and h_0), two can be estimated by independent means which do not involve the measured phase boundary for $\vec{H} \| [0001]$. We now present these independent estimates and show that they agree with the values which were obtained from the least-squares fits to Eq. (7).

TABLE III. Results of least-squares fits to Eq. (7) of the data for $\vec{H} \| [0001]$. A, B, and h_0 are treated as adjustable parameters, while ϕ is held fixed at its theoretical value $\phi(n=3) = 1.25$. For these fits, H and h_0 are in units of kOe, and T is in units of mK. The numbers in parentheses are standard deviations in units of the last quoted decimal place, e.g., 0.9743(1020) is 0.9743 ±0.1020, and 41.63(513) is 41.63 ±5.13. δT is the rms deviation (in mK) between the measured $T_c(H) - T_N$ and the best fit.

Sample No.	A	B	h_0	δT
1	0.9743(1020)	0.2051(119)	41.63(513)	2.87
2	1.0222(655)	0.2106(81)	44.40(251)	0.54

1. Estimate for h_0

The estimate for h_0 is based on an analogy with easy-axis antiferromagnets. In nearly all known easy-axis antiferromagnets (e.g., MnF_2,[29] Cr_2O_3,[30] $GdAlO_3$,[31] and $NiCl_2 6H_2O$[32]) the observed bicritical field H_b is within a factor of 2 of the spin-flop field at $T=0$, $H_{SF}(0) \cong (2H_E H_A)^{1/2}$. In most cases, the difference between H_b and $H_{SF}(0)$ is less than $\sim 30\%$. This feature is also obtained theoretically in the mean-field approximation if one considers the common types of easy-axis anisotropies. Examples of such mean-field calculations are given in Ref. 31. A simple extension of the mean-field calculations in Ref. 33, for single-ion anisotropy, also leads to the same conclusion. The essence of the mean-field result for H_b is given in the following order of magnitude estimate. Consider Fig. 10(a). The temperature difference $T_N - T_b$ is of order $T_N(H_A/H_E)$, where the exchange and anisotropy fields are measured at $T=0$. The slope $dT_c^{\parallel}/d(H^2)$ of the P-AF line in the $H^2 - T$ plane is of order $-T_N/H_E^2$. The same slope is also equal to $(T_b - T_N)/H_b^2$. Therefore, H_b is of order $(H_A H_E)^{1/2}$, which is of the same order of magnitude as $H_{SF}(0)$. The Monte Carlo results of Landau and Binder[11] suggest that the conclusion that H_b is comparable to $H_{SF}(0)$ is not peculiar to the mean-field approximation. On the experimental side, we are aware of only one material in which the spin-flop field H_{SF} changes with temperature by a large factor. The exceptional material is α-Fe_2O_3 which has rather unusual properties.[34]

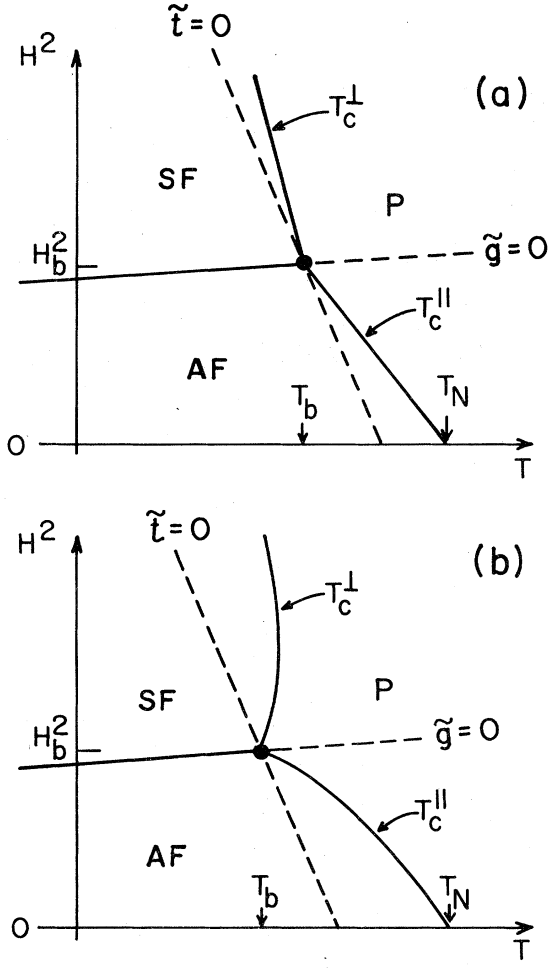

FIG. 10. Schematic of the phase diagram of an easy-axis antiferromagnet near the bicritical and Néel points. (a) Mean-field theory. (b) FNK theory. $\tilde{t}=0$ and $\tilde{g}=0$ are the optimal scaling axes (see text and Refs. 3, 28, and 35).

Based on the experience with easy-axis antiferromagnets we expect that also in the easy-plane antiferromagnet $CsMnF_3$, $H_{VB}^2 \equiv -h_0^2$ will be comparable to the square of the virtual spin-flop field at $T=0$. The latter is given by $H_{VSF}(0)^2 \cong -|2H_E H_A|$. The value of $H_{VSF}(0)^2$ can be deduced from antiferromagnetic resonance (AFMR) measurements. The AFMR frequency ω in an easy-plane antiferromagnet is given by[18,21]

$$(\omega/\gamma)^2 = |2H_E H_A| + H^2 \ , \tag{8}$$

where γ is the gyromagnetic ratio. The AFMR data of Borovik-Romanov *et al.*[18] give $H_{VSF}(0)^2 = -(41.1 \pm 0.6 \text{ kOe})^2$ for $CsMnF_3$. We therefore expect that h_0 will be comparable to 41 kOe. The actual values obtained by fitting the phase boundary for $\vec{H} \parallel [0001]$ to Eq. (7) are $h_0 = 41.6 \pm 5.1$ kOe for sample 1, and 44.4 ± 2.5 kOe for sample 2 (see Table III).

2. Estimate for B

The term $-BH^2$ in Eq. (7) is similar to a term in the FNK theory which appears as a result of choosing the optimal scaling axis $\tilde{t}=0$.[3,35] This scaling axis can be explained as follows. In the FNK theory the problem of the BP in an easy-axis antiferromagnet is reduced to the standard problem of crossover in anisotropic ferromagnets. To accomplish this reduction, it is necessary to measure temperatures relative to a scaling axis $\tilde{t}=0$ which passes through the BP, rather than relative to a fixed temperature $T_c(g=0)=T_b$ (see Fig. 10). This means that Eq. (5), which is based on standard extended scaling in ferromagnets, should be modified to account for the fact that temperatures are no longer measured relative to a fixed $T_c(g=0)$. The correction term for T_c is linear in H^2.

The optimal scaling axis $\tilde{t}=0$ for the VBP, and the correction term $-BH^2$ in Eq. (7), are similar to those in the theory for the ordinary BP. In addition, the term $-bH^2$ in Eq. (1), which describes the phase boundary near a "degenerate BP",[36] is also related to a similar optimal scaling axis. For $CsMnF_3$, we are

applying Eq. (1) to describe the phase boundary when $\vec{H}$ is in the (0001) plane, and Eq. (7) to describe the phase boundary for $\vec{H} \parallel [0001]$. We now show that B in Eq. (7) and b in Eq. (1) are theoretically related to each other, at least approximately. We then obtain an independent estimate for B in terms of b. Taking b from Tables I or II we obtain a numerical estimate for B which can be compared to the values for B obtained from the fits to Eq. (7).

An estimate for the slope $dT/d(H^2)$ of the scaling axis $\tilde{t}=0$ was given by Fisher.[3] This estimate is based on a mean-field calculation supplemented by certain renormalization-group results. The estimate is

$$\left(\frac{dT}{d(H^2)}\right)_{\tilde{t}=0} = \left(\frac{n+2}{3n}\right)\left(\frac{dT_c^{\parallel}}{d(H^2)}\right)_{\mathrm{MF}} , \tag{9}$$

where $[dT_c^{\parallel}/d(H^2)]_{\mathrm{MF}}$ is the slope of the P-AF boundary in the mean-field approximation,[37] and n is the number of critical spin components at the BP. The same estimate can also be written as

$$\left(\frac{dT}{d(H^2)}\right)_{\tilde{t}=0} = \left(\frac{n+2}{n}\right)\left(\frac{dT_c^{\perp}}{d(H^2)}\right)_{\mathrm{MF}} , \tag{10}$$

where $[dT_c^{\perp}/d(H^2)]_{\mathrm{MF}}$ is the slope of the P-SF boundary in the mean-field approximation. Our previous work on the cubic antiferromagnet $RbMnF_3$ (Ref. 13) suggests that the estimates (9) and (10) remain valid when the uniaxial anisotropy tends to zero and the BP becomes a degenerate BP.[36] That is, the estimate for the coefficient b in Eq. (1) is

$$b = -\left(\frac{dT}{d(H^2)}\right)_{\tilde{t}=0} = -\left(\frac{(n+2)}{n}\right)\left(\frac{dT_c}{d(H^2)}\right)_{\mathrm{MF}} , \tag{11}$$

where $[dT_c/d(H^2)]_{\mathrm{MF}}$ is the mean-field slope for the phase boundary near the degenerate BP. We expect Eq. (11) to hold also in the case of a degenerate BP with $n=2$.[36] That is, the coefficient b in Eq. (1) for the phase boundary when $\vec{H}$ is in the easy plane should be given roughly by Eq. (11).

Turning to the VBP, the coefficient B in Eq. (7) should be given by the expression on the right-hand side of Eq. (11), except that $n=3$ and $[dT_c/d(H^2)]_{\mathrm{MF}}$ is the mean-field slope of the (real) phase boundary when $\vec{H}$ is parallel to [0001]. For $CsMnF_3$, the latter mean-field slope is very nearly equal to the mean-field slope of the phase boundary for $\vec{H} \perp [0001]$. The percentage difference between the two slopes is of order $|H_A/H_E| \sim 1\%$. Thus the difference between the estimated values of B and b is almost entirely due to the change of the factor $(n+2)/n$ as n changes from 3 to 2. That is, the estimate for B is

$$B \cong \tfrac{5}{6} b \ . \tag{12}$$

From Tables I and II, $b=0.24$ mK/kOe^2, so that Eq. (12) gives $B \cong 0.20$ mK/kOe^2. The actual values for B obtained from fits of the phase boundary to Eq. (7), are 0.205 ± 0.012 and 0.211 ± 0.008 mK/kOe^2 (see Table III). Thus, the data agree with the estimate given by Eq. (12).

E. Conclusion

We now know of three types of bicritical points in cylindrically symmetric antiferromagnets: (i) the ordinary bicritical point, at a positive H^2, in easy-axis antiferromagnets; (ii) the degenerate bicritical point, at $H^2=0$, in fully isotropic antiferromagnets; and (iii) the virtual bicritical point, at a negative H^2, in easy-plane antiferromagnets. At all these bicritical points the net effective anisotropy (intrinsic anisotropy plus the H-induced effective anisotropy) is zero.

ACKNOWLEDGMENTS

We wish to thank D. R. Gabbe and A. Platzker for providing the samples, and V. Diorio for technical assistance. The Francis Bitter National Magnet Laboratory is supported by the NSF. This work was supported in part by a joint grant from the NSF (U.S.A.) and the Conselho Nacional de Desenvolvimento Cientifico e Technológico (Brazil).

---

*Also at Lyman Laboratory, Harvard Univ., Cambridge, Mass. 02138.

[1]L. Kadanoff, in *Critical Phenomena, Proceedings of the International School of Physics "Enrico Fermi", Course LI* (Academic, New York, 1971). See also reviews by H. E. Stanley and D. D. Betts, in *Phase Transitions and Critical Phenomena,* edited by C. Domb and M. S. Green (Academic, London, 1974), Vol. 3.

[2]M. E. Fisher and D. R. Nelson, Phys. Rev. Lett. 32, 1350 (1974).

[3]M. E. Fisher, Phys. Rev. Lett. 34, 1634 (1975), and in *Proceedings of the 20th Conference on Magnetism and Magnetic Materials, San Francisco, 1974,* edited by C. D. Graham, Jr., G. H. Lander, and J. J. Rhyne, AIP Conf. Proc. No. 24, (AIP, New York, 1975), p. 273.

[4]J. M. Kosterlitz, D. R. Nelson, and M. E. Fisher, Phys. Rev. B 13, 412 (1976).

[5]E. Riedel and F. Wegner, Z. Phys. 225, 195 (1969).

[6]P. Pfeuty, D. Jasnow, and M. E. Fisher, Phys. Rev. B 10, 2088 (1974).

[7]See, for example, A. Aharony, in *Phase Transitions and Critical Phenomena,* edited by C. Domb and M. S. Green (Academic, London, 1976), Vol. 6, and references therein.

[8]H. Rohrer, Phys. Rev. Lett. 34, 1638 (1975).
[9]N. F. Oliveira, Jr. and Y. Shapira, J. Appl. Phys. 50, 1790 (1979).
[10]Y. Shapira, N. F. Oliveira, Jr., and T. S. Chang, Phys. Rev. Lett. 42, 1292 (1979).
[11]D. P. Landau and K. Binder, Phys. Rev. B 17, 2328 (1978).
[12]Y. Shapira and C. C. Becerra, Phys. Rev. Lett. 38, 358, 733(E) (1977); Y. Shapira and N. F. Oliveira, Jr., J. Appl. Phys. 49, 1374 (1978).
[13]Y. Shapira and N. F. Oliveira, Jr., Phys. Rev. B 17, 4432 (1978).
[14]K. Lee, A. M. Portis, and G. L. Witt, Phys. Rev. 132, 144 (1963).
[15]V. Minkiewicz and A. Nakamura, Phys. Rev. 143, 361 (1966).
[16]L. B. Welsh, Phys. Rev. 156, 370 (1967).
[17]V. A. Tulin, Zh. Eksp. Teor. Fiz. 58, 1265 (1970) [Sov. Phys. JETP 31, 680 (1970)].
[18]A. S. Borovik-Romanov, B. Ya. Kotyuzhanskii, and L. A. Prozorova, Zh. Eksp. Teor. Fiz. 58, 1911 (1970) [Sov. Phys. JETP 31, 1027 (1970)].
[19]Y. Yamaguchi and T. Sakuraba, J. Phys. Soc. Jpn. 38, 1011 (1975).
[20]H. Ikeda, J. Phys. C 10, L469 (1977).
[21]E. A. Turov, *Physical Properties of Magnetically Ordered Crystals* (Academic, New York, 1965).
[22]A. A. Mil'ner and Yu. A. Popkov, Pis'ma Zh. Eksp. Teor. Fiz. 25, 244 (1977) [Sov. Phys. JETP Lett. 25, 225 (1977)].
[23]V. M. Gredeskul and A. A. Mil'ner, Fiz. Nizk. Temp. 4, 753 (1978) [Sov. J. Low Temp. Phys. 4, 359 (1978)].
[24]The basic design was discussed by G. K. White [Cryogenics 1, 151 (1961)]. The design of our dilatometer was slightly different, to allow measurements with insulating samples.
[25]Y. Shapira and N. F. Oliveira, Jr., Phys. Rev. B 18, 1425 (1978).
[26]A. D. Bruce and A. Aharony, Phys. Rev. B 11, 478 (1975).
[27]Y. Shapira (unpublished).
[28]More precisely, the optimal g is proportional to the difference between H^2 and the tangent to the virtual spin-flop line at the VBP (see Ref. 3). When the anisotropy is much smaller than the exchange energy, the slope of the virtual spin-flop line should be small enough to be ignored, and g should be very nearly proportional to H^2-H^2_{VB}.
[29]Y. Shapira and S. Foner, Phys. Rev. B 1, 3083 (1970).
[30]Y. Shapira, Phys. Rev. 187, 734 (1969).
[31]K. W. Blazey, H. Rohrer, and R. Webster, Phys. Rev. B 4, 2287 (1971).
[32]N. F. Oliveira, Jr., A. Paduan Filho, S. R. Salinas, and C. C. Becerra, Phys. Rev. B 18, 6165 (1978).
[33]Y. Shapira, Phys. Rev. B 2, 2725 (1970), Appendix.
[34]The phase boundaries of α-Fe_2O_3 were discussed, for example, by Y. Shapira [Phys. Rev. 184, 589 (1969)]. In α-Fe_2O_3 the small net uniaxial anisotropy is the result of two competing large uniaxial anisotropies of different physical origins and of different signs. [See J. O. Artman, J. C. Murphy, and S. Foner, Phys. Rev. A 138, 912 (1965)]. The small net uniaxial anisotropy has an unusually strong T dependence because the two competing anisotropies have different dependences on T. This leads to a strong T dependence of H_{SF}. In fact, the net uniaxial anisotropy of α-Fe_2O_3 changes sign as T crosses the so-called Morin temperature T_M. Thus, H_{SF} vanishes at T_M. This abnormal behavior of α-Fe_2O_3 is the exception rather than the rule.
[35]In the present case the other optimal scaling axis, $\tilde{g}=0$, can be taken as parallel to the T axis, as discussed in Ref. 28.
[36]An ordinary BP occurs in an easy-axis antiferromagnet when the anisotropy is small but finite. The term "degenerate BP" was used by Fisher (Ref. 3) to describe the situation when the uniaxial anisotropy tends to zero and the BP occurs at $H=0$. In a fully-isotropic three-dimensional antiferromagnet, $n=3$ at the degenerate BP. In the present paper we also use the term "degenerate BP" to describe the situation in an easy-plane antiferromagnet when: (i) the anisotropy in the easy plane tends to zero, and (ii) $\vec{H}$ is in the easy plane. In this case, $n=2$ at the degenerate BP.
[37]To make contact with experiment, Fisher took $[dT_c^{\parallel}/d(H^2)]_{MF}$ to be equal to the actual measured slope of the P-AF boundary at low H. However, this step is justified only when the uniaxial anisotropy is not too small, so that the BP is sufficiently far from the Néel point. Otherwise, the critical behavior near the Néel point is not free from the influence of the nearby BP, and the behavior near the Néel point is significantly different from mean-field behavior. This conclusion is consistent with the interpretation of the experimental findings in the low-anisotropy antiferromagnet Cr_2O_3 [Y. Shapira and C. C. Becerra, Phys. Rev. B 16, 4920 (1977)].